PHYSICAL REVIEW A VOLUME 10, NUMBER 6 DECEMBER 1974

Inelastic-scattering cross sections for Li^+ on He: The adiabatic molecular model

B. R. Junker
Department of Physics and Astronomy, University of Georgia, Athens, Georgia 30601

J. C. Browne
Departments of Computer Science and Physics, University of Texas, Austin, Texas 78712

(Received 18 June 1973; revised manuscript received 22 July 1974)

In this paper are reported *ab initio* computed cross sections for the two lowest charge-transfer channels and the lowest excitation channel for the system Li^+ scattered from He. The computations are carried out in completely *ab initio* fashion in the adiabatic molecular basis. The molecular potential curves and wave functions were computed by use of standard variational procedures. The coupling matrix elements between the molecular states are used in a classical trajectory formulation of the nuclear motion problem to obtain cross sections for the inelastic processes. The differential cross sections agree well with the experimental results of Lorents and Conklin and of Francois, Dhuicq, and Barat. The role of radial coupling in determining the charge-exchange cross sections is stressed.

I. INTRODUCTION

The discrepancy at small internuclear separations between the experimentally inferred ground-state potential curve for $^1\Sigma^+$ LiHe^+ obtained by Zehr and Berry[1] and the computed potential of Fischer[2] has led to several theoretical and experimental investigations of this system. Junker and Browne[3] computed a set of potential curves for the ground-state and low-lying excited states. The ground-state curve agreed well with that of Fischer. The computation of the excited-state curves revealed that the first excited $^1\Sigma^+$ state potential curve closely approached the potential curve of the ground $^1\Sigma^+$ state at around $R \simeq 0.5a_0$. This implied that inelastic channels should open when the energy of the Li^+ ion impinging on He was large enough so that the classical turning point in the collision would take place at $R \simeq 0.5a_0$. These inelastic processes have been experimentally studied by Lorents and Conklin,[4] who found energy-loss channels at 21 and 61 eV, which they interpret as belonging to excitation of $\mathrm{He}(1s2p, {}^1P)$ and excitation of doubly-excited He atom states. Francois, Dhuicq, and Barat[5] have carried out a similar set of measurements and have in addition obtained values for the charge-exchange cross sections which open at an energy loss of apparently just less than 21 eV. Park, Pal, Lawler, and George[6] have studied the excitation of $\mathrm{He}(2\,{}^1s)$ and $\mathrm{He}(2\,{}^1p)$ by 15–100-keV Li^+ ions. The charge-exchange process has also been investigated by Latypov and Shaporenko.[7] McCarroll and Piacentini[8] have carried out theoretical computations based upon a diabatic[9] model and the consideration of only rotational couplings between the diabatic states. Their computations thus ignore the possibility of the occurrence of the charge-transfer channel leading to $\mathrm{Li}(1s^22s, {}^2S)$.

In this paper we report the computation of the cross sections for the lowest excitation channel, $\mathrm{He}(1s2s, {}^1S)$ and the two lowest charge-transfer channels $\mathrm{Li}(1s^22s, {}^2S)$ and $\mathrm{Li}(1s^22p, {}^2P)$ in an adiabatic molecular basis. In this formulation the atoms and/or ions move in potentials defined by the adiabatic molecular potential curves and occupy a set of molecular states. Transitions between molecular states take place via rotational (Σ-Π) and radial (Σ-Σ) coupling of the adiabatic molecular states. The transition probabilities to atomic products are determined by the flux into the molecular channels separating into atomic products. (See Browne[10] for a thorough discussion of the adiabatic formulation).

The scattering cross sections were computed in an impact-parameter formulation with the nuclear motion determined by the ground-state potential. The basis for the cross-section computations included the four lowest molecular states: three states of Σ symmetry and one of Π symmetry. These cover the elastic channel, the lowest two charge transfer channels, and the lowest excitation channel. Rather good agreement with experiment is obtained. We find, contrary to McCarroll and Piacentini, that radial coupling is a significant factor. Computations were also carried out in a pair of two-state approximations: the two Σ states coupling the elastic channel and the lowest charge-transfer channel; and the ground state and the lowest Π state which is also a charge-transfer channel. This set of two-state computations were carried out to evaluate the relative significance of radial and rotational coupling in the adiabatic approximation.

II. WAVE FUNCTIONS AND MATRIX ELEMENTS

An approximate correlation diagram for the molecular system $LiHe^+$ is given as Fig. 1. This correlation diagram can be used as a basis for analyzing the set of molecular states which will be significant in computations leading to cross sections. Normally, only those states which cross or which lie close in energy will be sufficiently strongly coupled to produce transition probabilities between the sets of states. Note that the correlation diagram is a diabatic diagram. Thus, crossings shown in the correlation diagram among states of identical symmetry will become avoided crossings in the adiabatic picture. The lowest adiabatic states of a given symmetry at the separated atom limit pass smoothly to the lowest energy state of proper symmetry at the united atom limit. This is illustrated in Table I, where the adiabatic correlation of the seven lowest molecular states of the $LiHe^+$ system are listed. The correlation diagram shows that the lowest charge-transfer process [to $Li(1s^22s,{}^2S)$] can occur at an energy loss of approximately 19.2 eV. The first excitation to [$He(1s2s,{}^2P)$] opens at 20.61 eV. There exists in the experimental results a large energy-loss cross section at approximately 61 eV which is attributed to doubly excited states to the He atom. These channels cannot be included in the adiabatic calculations without resorting to stabilization[11] techniques. We therefore concentrate on the four lowest states accessible in the adiabatic approximation (and thus the lowest three inelastic channels) and base our computations upon these. It would have been desirable to include the Σ and Π molecular components of the $He(1s2p,{}^2P)$ channel. This would have greatly increased the complexity of the computations and the experiments do not at this time resolve the components of the charge-transfer and excitation channels.

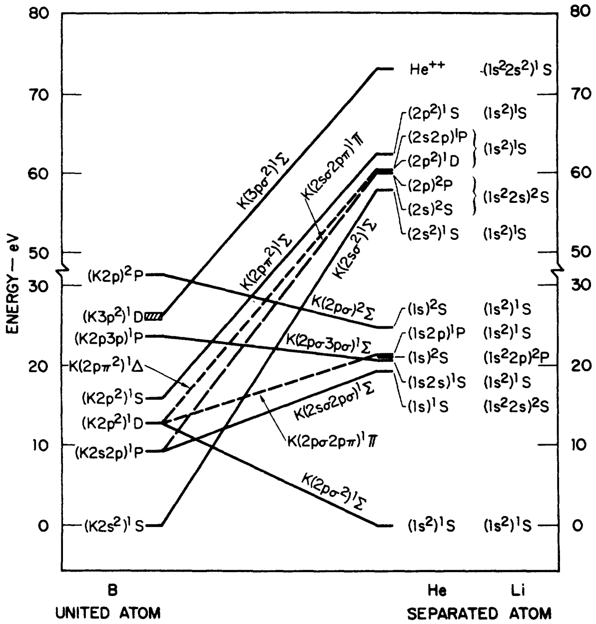

FIG. 1. Diabatic correlation diagram for the molecular system $LiHe^+$ (Taken from Lorents and Conklin, Ref. 4).

Each molecular wave function and state was represented by a generalized valence-bond configuration-interaction wave function which contained united-atom terms, separated-atom terms, and terms to deal with electron correlation. Some of these terms have negligible contribution at either the separated-atom limit or the united-atom limit and are thus removed from the wave function when their coefficients become small. Over most of the range of internuclear separations, the ground-state $^1\Sigma^+$ wave function used contained 30 configurations including 6 elliptic orbital configurations corresponding to united-atom states to provide good potential-energy curve characteristics at small internuclear separations. The lowest $^1\Sigma$ excited state corresponding to separation into $Li(1s^22s,{}^2S)+He^+(1s,{}^2S)$, had up to 16 configurations including 4 configurations compounded from elliptic orbitals chosen to represent effectively the united-atom region of internuclear separation. The second excited state of $^1\Sigma$ character [separa-

TABLE I. Adiabatic correlation of molecular states.

State	Separated-atom limit	Energy loss to state	United-atom limit
$^1\Sigma^+(1)$	$Li^+(1s^2,{}^1S)+He(1s^2,{}^1S)$		$B^+(1s^2,2s^2,{}^1S)$
$^1\Sigma^+(2)$	$Li(1s^22s,{}^2S)+He^+(1s,{}^2S)$	19.1	$B^+(1s^2,2s2p,{}^1P)$
$^1\Sigma^+(3)$	$Li^+(1s^2,{}^1S)+He(1s2s,{}^1S)$	20.61	$B^+(1s^22p^2,{}^1D)$
$^1\pi(1)$	$Li(1s^22p,{}^2P)+He^+(1s,{}^2S)$	21.04	$B^+(1s^22s2p,{}^1P)$
$^1\Sigma^+(4)$	$Li(1s^22p,{}^2P)+He(1s,{}^2S)$	21.04	$B^+(1s^22p^2,{}^1S)$
$^1\pi(2)$	$Li^+(1s^2,{}^1S)+He(1s2p,{}^1P)$	21.2	$B^+(1s^22p^2,{}^1D)$
$^1\Sigma^+(5)$	$Li^+(1s^2,{}^1S)+He(1s2p,{}^1P)$	21.2	$B^+(1s^22s3s,{}^1S)$

ting to $Li^+(1s^2, {}^1S) + He(1s2s, {}^1S)$] utilized a 22 configuration wave function similar to that used for the first $^1\Sigma$ excited state. The lowest Π state separating to $Li(1s^2 2p, {}^2P) + He^+(1s, {}^2S)$ was represented by an 8 configuration wave function with two elliptic orbital configurations being used to give a good representation of the potential-energy curve near the united-atom limit. Considerable stress was placed on good potential curve representations close to the united-atom limit because of our interest in exploring the significance of the radial couplings which occur at the avoided crossings at very small distances.

In each case all of the orbital exponents were chosen to minimize the energy at each internuclear separation. That is, the ground-state wave function was taken to have up to 13 independent nonlinear parameters which were chosen to minimize the energy. The first and second excited $^1\Sigma$-state wave functions had up to 10 nonlinear parameters and the first excited $^1\Pi$-state wave function had up to 8 nonlinear parameters. The computations were carried out with the programs and procedures of the Molecular Physics Group at the University of Texas at Austin. The numerical potential curves are given as Table II. Electronic potential energies are plotted as Fig. 2. All three $^1\Sigma^+$ potential curves have small minima. The ground state shows a minimum of 0.00109 a.u. at $R = 3.85a_0$, while the first excited $^1\Sigma^+$ potential curve shows a minimum of 0.0572 a.u. at $R = 6.47a_0$. The depth of the potential for the $^1\Sigma$ first excited state is approximately 50 times that of the ground state. This leads to the interesting result that the two states of $^1\Sigma$ symmetry approach very closely at an internuclear separation of about $R = 0.5a_0$ and remain very close until very near the united-atom limit.

The potential-energy curve for the ground state is by far of the highest absolute accuracy yet reported. It agrees well with the relative interaction energies obtained by Fischer and is in relatively good agreement with the curve obtained by Olson, Smith, and Mueller[12] from analysis of the data of Aberth and Lorents.[13] It does not, however, provide a really accurate description of the long-range interaction. Catlow[14] *et al.* have recently considered in detail the long range form of the potential curve and its effects on the elastic-scattering cross section of the ground-state potential.

III. REDUCED DIFFERENTIAL CROSS SECTIONS

A pair of two-state impact-parameter cross-section calculations were performed: one coupling the ground $^1\Sigma$ and the first excited $^1\Sigma$ (lowest charge transfer) excited channel and another coupling the ground $^1\Sigma$ and $^1\Pi$ (second lowest charge-transfer channels). The purpose of these computations was to determine the relative signifi-

TABLE II. Electronic energies of molecular states.

$R\,(a_0)/[-E\,(\text{a.u.})]$	$^1\Sigma^+(1)$	$^1\Sigma^+(2)$	$^1\Sigma^+(3)$	$^1\pi$
25.0	10.411 98	9.704 79	9.648 50	9.637 49
20.0	10.471 98	9.765 14	9.710 23	9.697 18
15.0	10.571 98	9.866 44	9.816 09	9.796 32
12.0	10.671 99	9.969 07	9.920 57	9.894 91
10.0	10.772 01	10.072 89	10.017 27	9.992 81
8.0	10.922 14	10.227 73	10.153 82	10.138 25
7.0	10.029 33	10.335 10	10.249 41	10.241 09
6.0	11.172 35	10.466 65	10.376 02	10.375 54
5.5	11.263 34	10.555 95	10.455 99	10.462 68
5.0	11.372 62	10.652 08	10.551 20	10.564 89
4.5	11.506 16	10.765 79	10.667 35	10.688 83
4.0	11.673 04	10.905 09	10.809 60	10.842 39
3.5	11.886 98	11.084 05	10.987 53	11.037 80
3.0	12.168 84	11.323 66	11.223 59	11.294 81
2.5	12.550 20	11.662 54	11.553 83	11.646 49
2.0	13.074 77	12.161 74	12.035 03	12.148 45
1.75	13.421 58	12.500 45	12.350 16	12.482 64
1.50	13.825 81	12.926 98	12.758 01	12.892 32
1.25	14.306 82	13.476 52	13.256 33	13.397 60
1.0	14.915 02	14.218 28	13.875 04	14.060 84
0.75	15.772 86	15.315 00	14.721 20	14.977 07
0.50	17.232 57	17.137 56	16.836 90	16.769 50
0.25	20.289 48	20.285 36	20.176 56	20.209 24
0.15	22.281 15	22.000 90	21.873 87	21.957 39

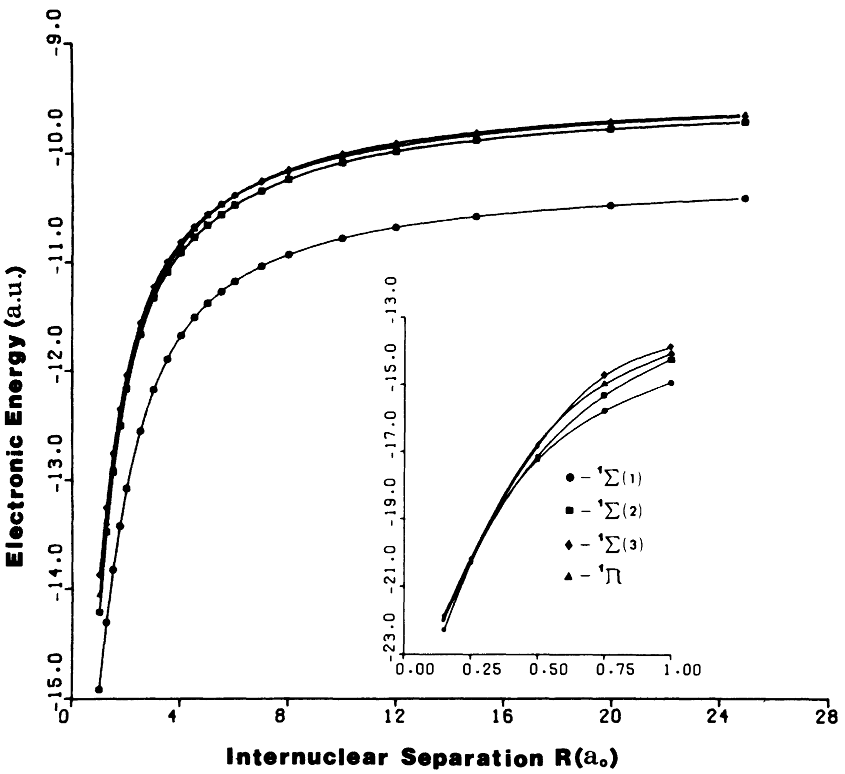

FIG. 2. Electronic potential-energy curves for the three lowest $^1\Sigma$ states of LiHe$^+$ and the lowest $^1\pi$ state of LiHe$^+$.

cance in our basis set of the radial (Σ-Σ) coupling versus the rotational (Σ-Π) coupling. The diabatic model of McCarroll and Piacentini assumes that there should be no direct flux into the Li($1s^22s$, ^2S) channel, and places the lowest direct charge-transfer channel at the Li($1s^22p$, ^2P) channel. The adiabatic model used in the present computations allows both channels to be directly populated from the ground-state channel.

The calculated reduced differential cross sections, $P = \theta \sin\theta\ \sigma(\theta)$, from these two-state models are indicated by the points in Fig. 3, while the lines are smooth curves drawn to connect the points. The Li($1s^22s$, ^2S) cross section (resulting from Σ-Σ coupling) is very large, particularly at the lowest energy and exhibits some oscillatory structure at the higher energies. The cross sections for Li($1s^22p$, ^2P) (Σ-Π coupling) are approximately two orders of magnitude smaller at the lowest energies and still considerably smaller at the higher energies although its magnitude increases as would be expected.

The reduced differential cross sections for the above two channels from the four-state model are illustrated in Fig. 4. The value of the total charge-transfer cross section at the first maximum agrees to within 10% of that of Lorents and Conklin at 1.5 and 2 keV and is about 40% higher at 1 keV. It is approximately twice as large as the results of Francois, Dhuicq, and Barat. The relative shape of the cross section, however, is very good. The location of the maxima agrees to within 2 keV degrees for all energies. These results strongly suggest that the radial coupling is a very important mechanism and that experiments with sufficient resolution in energy loss would be able to detect separate peaks for the onset of the two lowest charge-transfer channels. The experiments of Francois, Dhuicq, and Barat do indicate that the onset of the charge-exchange reaction occurs at a lower value of γ $(=E\theta)$ than does the onset of the 21 eV excitation process. This would be due to radial coupling. Park, Pal, Lawler, and George have carried out experiments at higher energies. The resolution in these experiments is approximately 0.5 eV. These authors attribute approximately 40% of the observed peak to the 20.611 eV energy loss due to He($2\,^1S$) excitation. They also believe that the same mechanism is operative at these higher energies as at the lower energies of the experiments of Lorents and Conklin, and Francois, Dhuicq, and Barat.

Several features are noteworthy upon comparing the two- and four-state models. First, in the four-state model the cross sections for the Li($1s^22p$, ^2P) charge exchange becomes larger than that for the Li($1s^22s$, ^2S) channel above 1 keV. The oscillatory structure of the Li($1s^22s$, ^2S) chan-

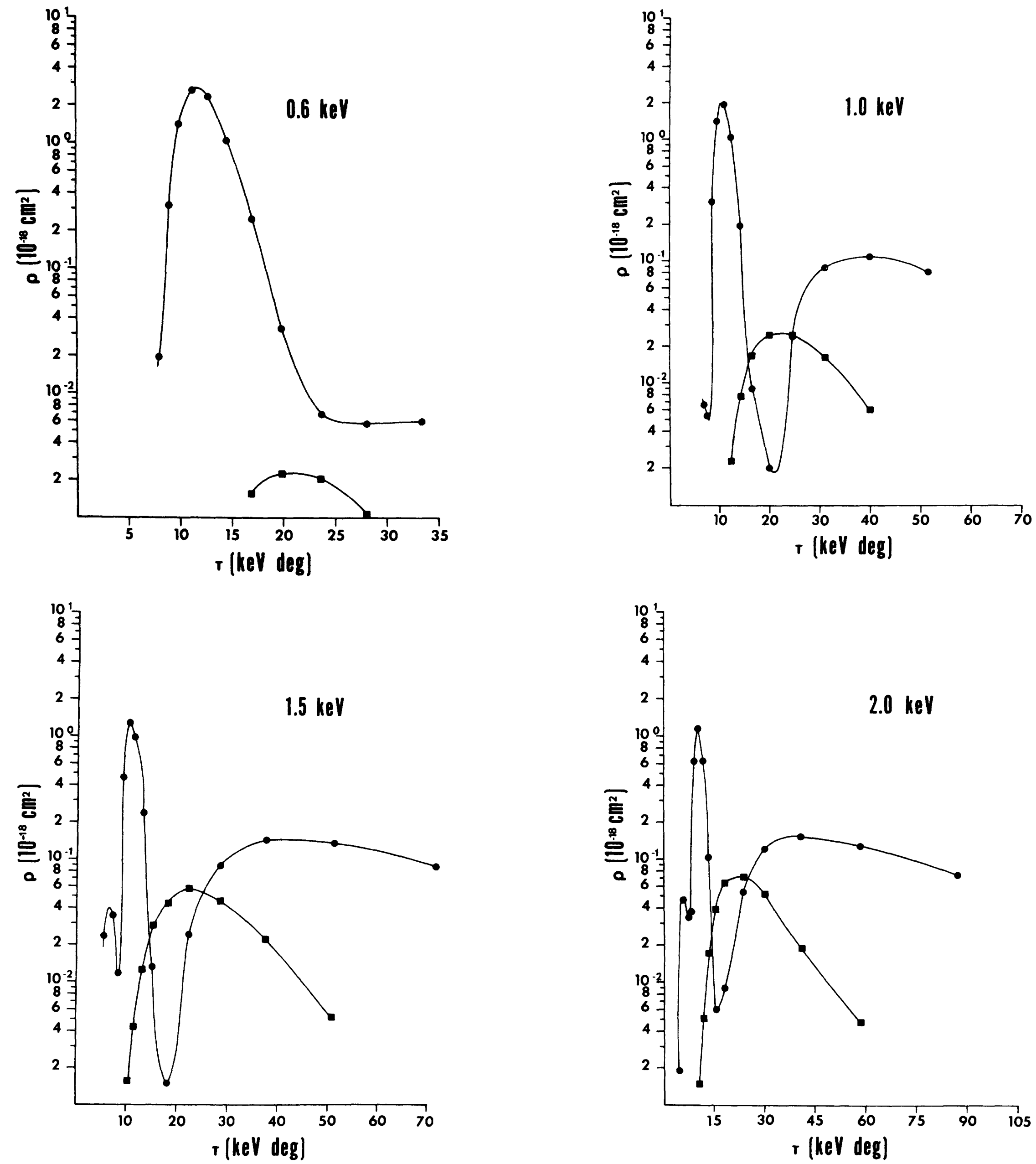

FIG. 3. Calculated reduced differential charge-transfer cross section from two-state models of the collision process. ●, $Li^+ + He \rightarrow Li\ (2s, {}^2S) + He^+\ (1s, {}^2S)$; ■, $Li^+ + He \rightarrow Li\ (2p, {}^2P_a) + He^+\ (1s, {}^2S)$.

nel has been markedly altered. It is significant that when one considers the total charge-transfer cross section the oscillatory structure in the region of the experimental data is no longer observable.

The theoretical reduced differential cross sections for the He$(1s2s, {}^2S)$ excitation channel are compared in Fig. 5 with the 21-eV energy loss channel of Lorents and Conklin. Although the location of the experimental and theoretical maxima around 10 keV deg agrees very well, the magnitudes differ by approximately a factor of 2. Both Lorents and Conklin and Francois, Dhuicq, and Barat believe the 21-eV loss peak to result predominately from the He$(1s2p, {}^1P)$ channels. The appearance of the second maximum around 25 keV deg in

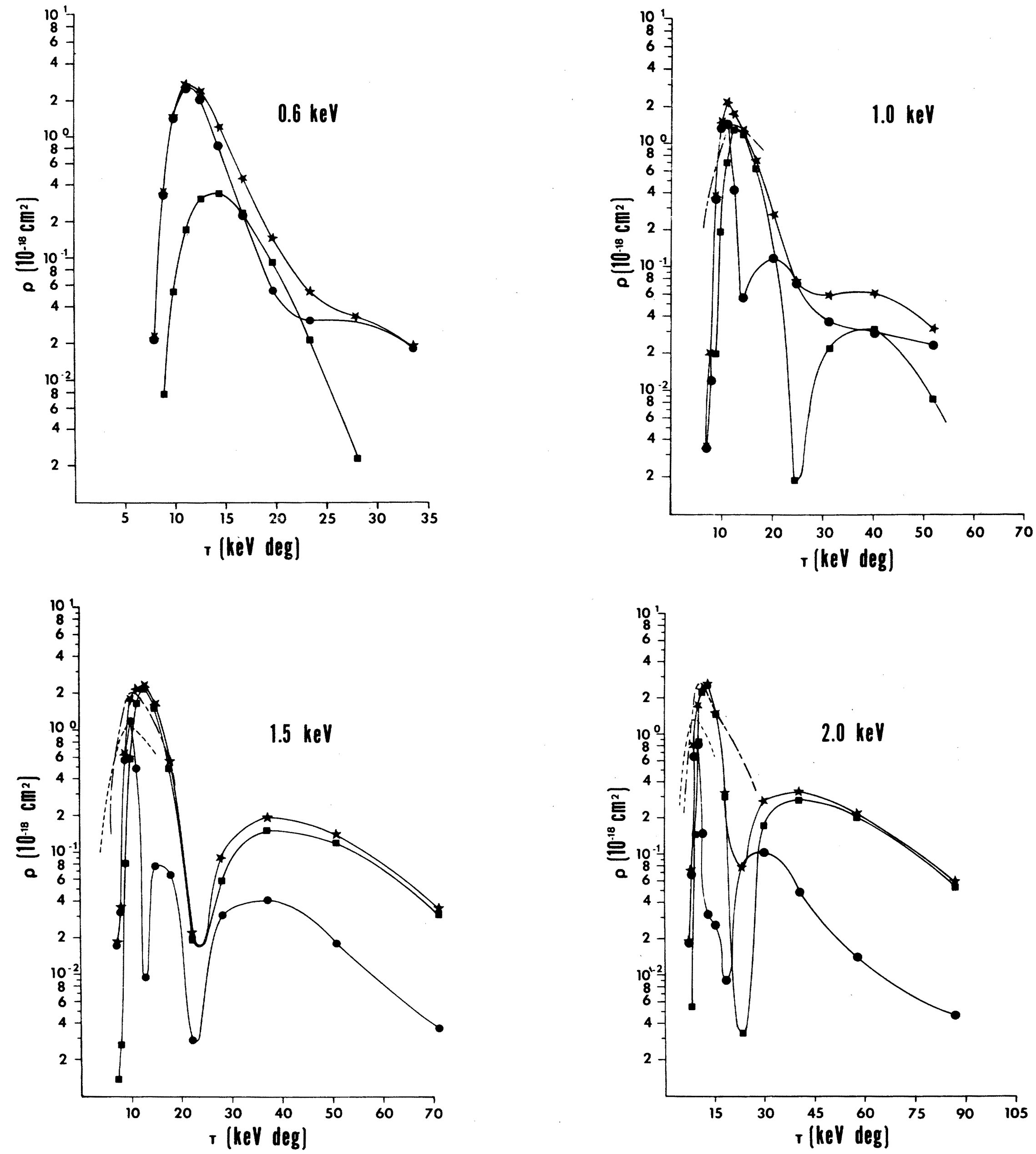

FIG. 4. Calculated reduced differential charge-transfer cross sections from the four-state model of the collision process. ●, $Li^+ + He \rightarrow Li\ (2s, {}^2S) + He^+\ (1s, {}^2S)$; ■, $Li^+ + He \rightarrow Li\ (2p, {}^2P_a) + He^+\ (1s, {}^2S)$; ★, calculated total charge-transfer cross section; ---, total charge-transfer cross section of Francois *et al.*, Ref. 5; ----, total charge-transfer cross sections of Lorents and Conklin, Ref. 4.

the theoretical cross sections may result from the lack of the double excitation channels in the theoretical model. (In order to conserve flux, the probability of excitation at higher energies must go into the existing channels.) Toward higher energies this second theoretical maxima drops below the experimental results which may be evidence of the emerging importance of the rotational coupling to states such as $He(2s2p, {}^1P)$, $He(2p^2, {}^1D)$ which were not included in this computation. In

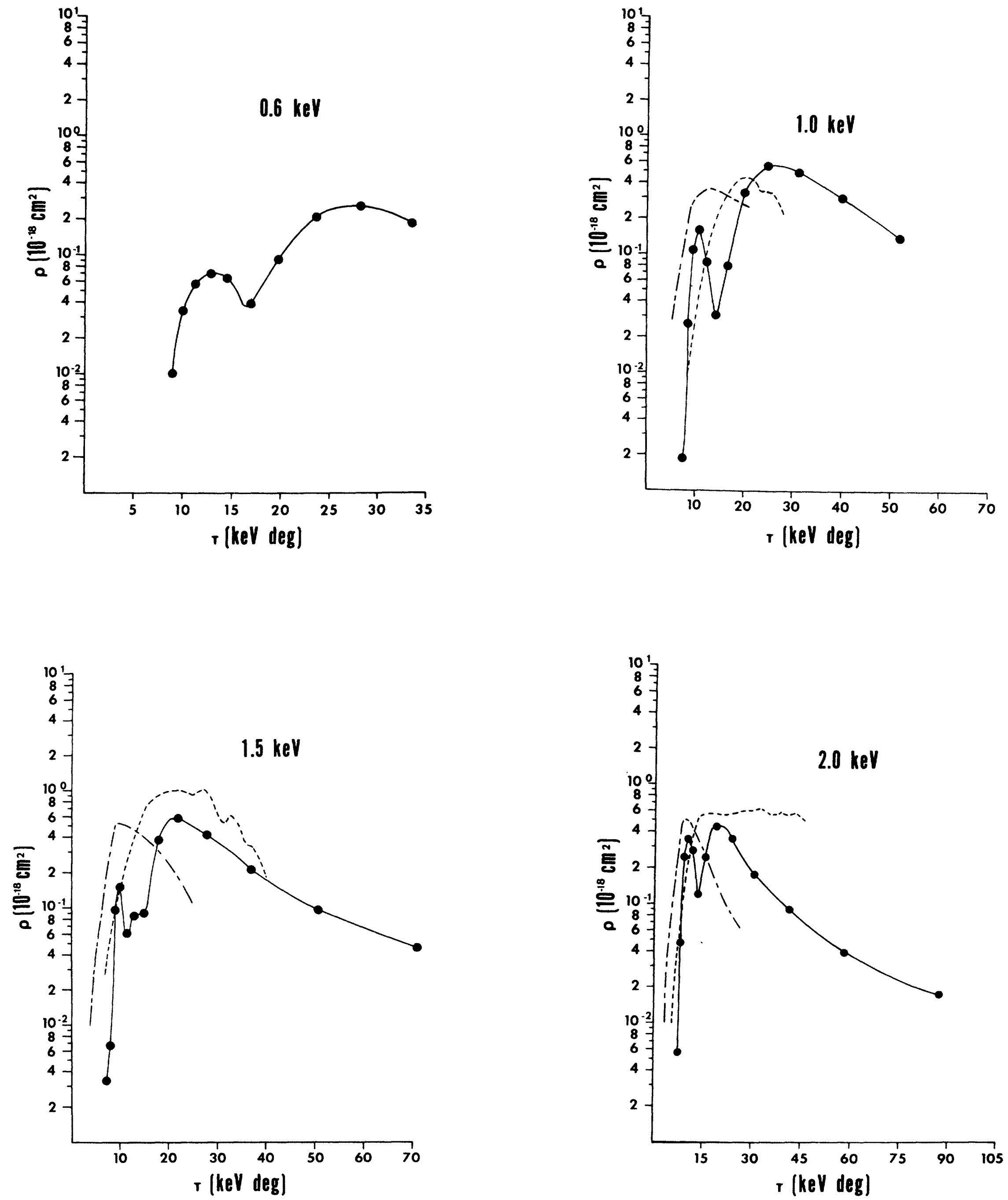

FIG. 5. Calculated reduced differential excitation-transfer cross sections, $Li^+ + He \rightarrow Li^+ + He\ (1s2s, {}^1S)$. ●, calculated cross section; ---, experimental, Lorents and Conklin, Ref. 4, 21.2 eV loss; ----, experimental, Ref. 4, 58.5 eV loss.

Fig. 6 the total charge-transfer cross sections from this computation and several experimental determinations are compared. At the lower energies we agree to within 10% with results of Lorents and Conklin, whereas at higher energies the shape of the theoretical curve agrees better with the results of Francois, Dhuicq, and Barat, although their curve is approximately 20% lower than ours.

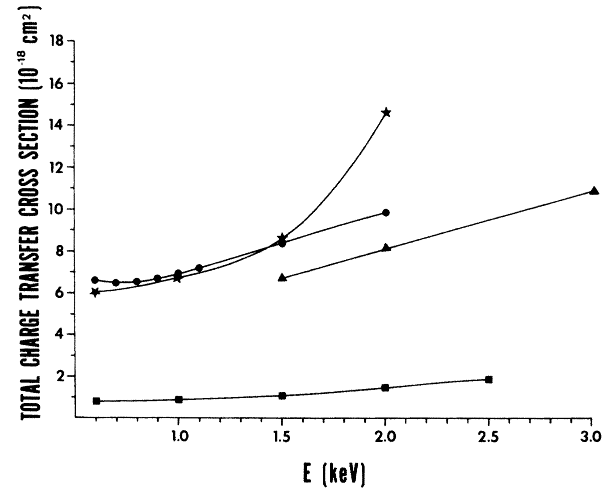

FIG. 6. Total charge-transfer cross sections as a function of energy in keV. ●, calculated; ■, Latypov and Shaporenko, Ref. 7; ▲, Francois, *et al.*, Ref. 5; ★, Lorents and Conklin, Ref. 4.

The total charge-transfer cross sections as a function of energy are given in Fig. 6. The total cross sections for each process are given as a function of energy in Table III.

IV. NEEDED EXTENSIONS TO THE CROSS-SECTION COMPUTATION

The results given here strongly suggest that the radial coupling into the Li($1s^2 2s$, ^2S) charge-transfer channel is quite large, indicating that the Σ-Σ coupling mechanism is important in the lower energy-loss charge-transfer channels. This is also suggested by the higher-energy experiments by Park, *et al.* Note that since the separated atom pair Li$^+$($1s^2$, ^1S) and He($1s^2$, ^1S) correlates diabatically to the B$^+$($1s^2 2p^2$, $1s$) and B$^+$($1s^2 2p^2$, ^1D) united atom states and since the separated atom pairs Li$^+$($1s^2$, ^1S) and He($2s^2$, ^1S), and Li$^+$($1s^2$, ^1S) and He($2p^2$, ^1D) correlate diabatically to the B$^+$($1s^2 2s^2$, ^1S) and B$^+$($1s^2 2p^2$, ^1D) states, respectively, the adiabatic model generates a large number of avoided crossings. Consequently, the path to the 61-eV excitation is through Σ-Σ, Σ-Π, and Σ-Π-Δ couplings with the latter becoming more important toward higher energies. The large coupling between the Σ states in the adiabatic model is responsible for the large flux into the Li($1s^2 2p$, ^2P), as comparison of Figs. 3 and 4 indicates. It is also responsible for the change in the oscillatory structure of the cross sections for the Li($1s^2 2s$, ^2S) channel between the two-state and four-state computations. This loss of structure points out the difficulty and danger which can arise in attempting to interpret experimental data in terms of excessively simple models when several channels are important. The increasing oscillatory structure of the 61-eV excitation of Lorents and Conklin may be the result of the increasing number of channels which lead to the 61-eV energy-loss process as the impact energy increases. This is clearly a system where increasing higher-resolution experiments and computations can go hand in hand to produce an improved model of the physical processes involved.

TABLE III. Total cross sections (10^{-17} cm^2).

Energy (eV)	Li($1s^2 2s$, ^2S) + He$^+$($1s$, ^2S)	Li($1s^2 2p$, ^2P) + He$^+$($1s$, ^2S)	Li($1s^2$, ^1S) + He($1s2r$, ^1S)
600	0.560	0.102	0.0959
700	0.468	0.175	0.177
800	0.400	0.250	0.235
900	0.348	0.317	0.281
1000	0.309	0.384	0.292
1100	0.276	0.444	0.300
1500	0.201	0.642	0.294
2000	0.180	0.806	0.275

ACKNOWLEDGMENTS

This research was supported by the Robert A. Welch Foundation of Houston, Texas and by the Office of Naval Research under contract N00014-67-A-0126-0017. The authors gratefully acknowledge the discovery by Don Lorents of a major conceptual error in an earlier version of this manuscript.

---

[1] R. J. Zehr and H. W. Berry, Phys. Rev. 159, 13 (1967).

[2] C. R. Fischer, J. Chem. Phys. 48, 215 (1968).

[3] B. R. Junker and J. C. Browne, *Proceedings of the Sixth International Conference on the Physics of Electronic and Atomic Collisions* (MIT Press, Cambridge, Mass., 1969), pp. 220-222.

[4] D. C. Lorents and G. M. Conklin, J. Phys. B 5, 950 (1972). In these experiments only energy losses to neutral excited states of He could be observed.

[5] R. Francois, D. Dhuicq, and M. Barat, J. Phys. B 5, 963 (1972).

[6] J. T. Park, V. Pol, J. Lawler and J. George, Phys. Rev. 30, 1013 (1973).

[7] Z. Z. Latypov and A. A. Shaporenko, *Proceedings of the Seventh International Conference on Physics of Electronic and Atomic Collisions* (Amsterdam, North-Holland, 1971), p. 138.

[8] R. McCarroll and R. D. Piacentini, J. Phys. B 5, 973

(1972).

[9] W. Lichten, Phys. Rev. 131, 229 (1963).

[10] J. C. Browne, Adv. Atom. Mol. Phys. 7, 47 (1971).

[11] H. S. Taylor, G. V. Nazaroff, and A. Gobeliewski, J. Chem. Phys. 45, 2872 (1966).

[12] R. E. Olson, F. T. Smith, and C. R. Mueller, Phys. Rev. A 1, 27 (1970).

[13] W. Aberth and D. C. Lorents, Phys. Rev. 182, 162 (1969).

[14] G. W. Catlow, M. R. C. McDowell, J. J. Kaufman, L. M. Sachs, and F. S. Chang, J. Phys. B 3, 833 (1970).